Fluorescent Probe Studies of the Association in an Aqueous Solution of a Hydrophobically Modified Poly(ethylene oxide)

Olga Vorobyova, Ahmad Yekta,† and Mitchell A. Winnik*

Department of Chemistry, University of Toronto, Toronto, Ontario, Canada M5S 3H6

Willie Lau

Research Laboratories, Rohm and Haas Company, Spring House, Pennsylvania 19477

Received May 22, 1998; Revised Manuscript Received August 24, 1998

ABSTRACT: We have used pyrene fluorescent probe experiments to study aqueous solutions of a poly(ethylene oxide) (PEO) of $M = 35000$ with $C_{16}H_{33}$ end groups. The end groups were attached by reaction of the PEO with hexadecyl isocyanate, and the polymer was then purified so that essentially all of the polymer in the sample contained 2.0 end groups/polymer molecule. The hydrophobic end groups of this polymer associate in water to form micelle-like structures which serve as solubilization sites for the pyrene molecules. Fluorescence decay profiles for both pyrene and 1-ethylpyrene were fitted to the Poisson quenching model to obtain the parameters n, the mean number of quenchers per micelle, and k, the pseudo-first-order rate constant for the quenching reaction in the micelle. While the data seem relatively well-behaved, we obtain different values for the end-group aggregation number (N_R) for the two probes. For ethylpyrene, $N_R = 16$ and $k = 10.4\ \mu s^{-1}$, while for pyrene, $N_R = 21$ and $k = 8.7\ \mu s^{-1}$. Plots of n versus [Py] or [EtPy] are linear for various polymer concentrations, but exhibit a nonzero intercept in the limit of low quencher concentration. We examine a number of possible explanations for this behavior.

Introduction

Associative thickeners (ATs) are members of a class of water-soluble polymers that contain hydrophobic substituents.[1] When these polymers are added to water in small amounts, the viscosity increases and the solution "thickens", giving the name to this class of polymers. The feature of these polymers that makes them interesting from an industrial point of view is their viscosity profile at different shear rates. ATs are used as rheology modifiers in water-born coatings such as paints and paper coatings, in adhesives and sealants, and in oil-recovery applications.[2] The field of applications is expanded by the sensitivity of the rheological behavior to the chemical structure of the polymer, the nature of the hydrophobic substituent, and the number of hydrophobes per polymer. As a consequence, there is a deep and growing interest in the underlying science of polymer association in aqueous solution. We now appreciate that these polymers in water associate through local phase separation of the hydrophobic groups into micelle-like structures. The polymer backbone forms bridges between micelles, and in this way the polymer self-assembles to form a transient network.[3,4]

Of the various associative polymers that have been studied, we have the deepest understanding of the telechelic associating polymers. These are linear water-soluble polymers, normally poly(ethylene oxide) (PEO), with hydrophobic end groups. Such polymers have been studied by a variety of techniques including rheometry, small-angle scattering (SANS and SAXS) measurements,[5,6] calorimetry, electron paramagnetic resonance (EPR) spectroscopy,[7] and fluorescence.[8−10] A recent theoretical paper predicted that this kind of polymer would undergo a special transition in their associative structure.[11] These types of polymers were predicted to form flower (or rosette) micelles at low polymer concentrations. Because these flower micelles should have weak attractive interactions with no repulsive interactions beyond the hard-sphere separation, they were predicted to phase separate from dilute solution into a polymer-rich phase of weakly bridged micelles. Flower micelles have been inferred from light scattering and by pulsed gradient NMR in two telechelic AT systems in water,[12] and in organic solvents for various triblock copolymers with insoluble end blocks.[13,14] We now also appreciate that if the substituents are not sufficiently hydrophobic, so that the onset of association (the critical aggregation concentration, CAC) is too high, there may be no concentration range preceding the formation of extended networks where discrete flower micelles can exist.[15]

For AT polymers, one of the most important morphological features one needs to characterize in order to describe the system properly is the number of hydrophobic substituents, N_R, that associate to form a micelle. N_R is an aggregation number analogous to that (N_{agg}) used to describe the number of surfactant molecules per micelle for simple surfactants in water. For many surfactant micelles, N_{agg} has values of 60−100 molecules/micelle. For the micelle-like structures formed by telechelic associating polymers, the N_R values are smaller, typically 15−30 end groups/micelle, and they are more difficult to determine. As a consequence they are known with much less confidence.

Our group used pyrene as a fluorescent probe to determine N_R values for a set of hydrophobe-modified ethoxyated urethane (HEUR) polymers with $C_{16}H_{33}O-$ end groups.[9] HEUR polymers are prepared by reacting

* To whom correspondence should be addressed. E-mail: mwinnik@chem.utoronto.ca.

† Current address: Imaging Research Inc., 500 Clenridge Ave., Brock University, St. Catarines, Ontario, Canada L2S 3A1.

10.1021/ma980819l CCC: $15.00
Published on Web 11/19/1998

oligomeric PEO chains with a diisocyanate to elongate the chain and to permit attachment of the end groups. In the system previously studied, isophorone diurethane (IPDU) groups are used to attach the $C_{16}H_{33}O-$ unit and an IPDU becomes part of the total hydrophobic end group. We found N_R values ranging from 20 to 28 for several similar polymers differing in chain length (M_n = 34000−51000), but for any one polymer, the value of N_R did not change over a limited range of concentrations that spanned flower micelles to well-formed networks. This result leads one to conclude that the system follows a closed association model for micelle core formation over this concentration range.

Persson et al.[7] used electron paramagnetic resonance (EPR) spectroscopy to determine the N_R value for a PEO polymer of M = 9300 with $C_{12}H_{25}$ groups attached to the chain ends by an ether linkage. Like the fluorescence quenching technique, the EPR approach assumes a Poisson distribution of spin probes among micelles. In this way the authors determined that $N_R = 31 \pm 6$ at a polymer concentration of 2.5 wt %. Similar polymers were examined by SAXS and SANS by the group of J. François in France. These polymers form an ordered phase at high concentrations (>20 wt %).[5,6] Under these circumstances, values of N_R can be estimated from the scattering data. In the context of the model they used to fit the data, the values of N_R appeared to increase with the increasing polymer concentration. Some information is available on aggregation numbers in flower micelles. Assuming hard-sphere behavior for these objects, one can combine intrinsic viscosity data with diffusion coefficients determined by dynamic light scattering (DLS) or pulsed-gradient spin−echo NMR to calculate the mean number of polymer molecules per flower micelle. In this way an N_R value of 30 was estimated for a PEO polymer of M = 35000 with $C_8F_{17}O-$ end groups, each coupled to the chain end via an IPDU group.[16]

In a recent publication, Alami et al.[17] reported fluorescence quenching measurements to determine N_R values for a $C_{12}H_{25}$ end-capped PEO of M = 20000 using two different quenchers. Using pyrene as a probe and dimethylbenzophenone as a quencher, they found an aggregation number of 28 ± 3 for polymer concentrations from 2 to 7 wt %. In the same work, quenching by pyrene excimer formation leads to very different aggregation numbers (16) for a 6 wt % polymer solution. To explain this difference, the authors expressed their concern about the validity of the Poisson distribution of fluorophores and quenchers in the micelle-like structures formed by their polymer.

The fluorescence quenching method was originally developed in the late 1970s for characterizing low-molecular-weight surfactants.[18] Since then, it has become the method of choice for determining surfactant aggregation numbers in water.[19,20] Novel developments with this technique that extend it to more complicated systems by considering polydispersity effects, different geometries, and dynamic aspects of the micelles have been reviewed recently.[21] Nevertheless, the probe dependence of the N_R values found by Alami et al.[17] is rather disconcerting. It may be that the entire strategy of using fluorescence quenching experiments to elucidate the size of the micelle-like structures formed in water by polymer-bound hydrophobic substituents needs to be reexamined.

In the present paper, our objective is to take a well-defined polymer sample and use it as a "test platform" to examine pyrene excimer formation as a way of obtaining aggregation numbers. We compare pyrene (Py) itself with 1-ethylpyrene (EtPy) as fluorescent probes. The polymer we examine (HDU), whose structure is shown below, is a well-characterized model material, a linear poly(ethylene oxide) with a molecular weight of 35000, and end-capped with hexadecyl (C_{16}) alkyl chains attached at both ends through reaction with hexadecyl isocyanate. In this study we determine the aggregation numbers in micelles formed by HDU for a broad range of polymer concentrations and fluorescent probe concentrations.

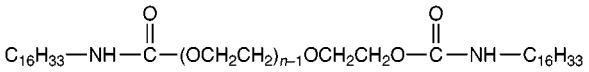

HDU $n = 800$

Experimental Section

Materials. The associative polymer used in this study (HDU) was synthesized at Rohm and Haas. A mixture of poly(ethylene oxide) (150 g, M_W = 35000, Fluka) and toluene (300 g) were predried by azeotropic distillation. The mixture was cooled to 80 °C and hexadecyl isocyanate (2.1 g, Carbolabs Inc.) was added, followed by dibutyl tin dilaurate (0.2 g). The reaction mixture was kept at 80 °C and monitored by IR for persistence of the isocyanate. Two additional shots of hexadecyl isocyanate (2.1 and 2.7 g, respectively) were added until a distinct excess of isocyanate was observed by IR. Hexanol (2 g) was then added to react with the excess isocyanate. After the solution cooled to room temperature, toluene was removed under vacuum. The resulting polymer was recrystallized from a mixture of THF and hexane. The molecular weight of the product was determined with size-exclusion chromatography, using a Perkin-Elmer HPLC equipped with a Waters 410 differential refractometer and two columns, Progel TSK G3000 HXL and G4000 HXL. Standard poly(ethylene oxide) samples from Polymer Laboratories were used for calibration. THF was used as the elution solvent at 40 °C. The molecular weight of the HDU polymer was found to be 35300, with a polydispersity index M_w/M_n = 1.10.

Aqueous solutions of this polymer contain a white water-insoluble impurity that interferes with all spectroscopic and scattering measurements. For concentrations below 2 wt % this impurity can be removed by filtering the polymer solution through a 0.8-μm filter, although the high viscosity of the solutions makes the filtering very difficult. To overcome this problem, HDU was dissolved in methanol (10−15 wt %). The resulting solutions were opaque but could be easily filtered through a 0.65-μm cellulose acetate filter. The filtrates were clear. After filtration, methanol was removed on a rotary evaporator under vacuum. It is likely that the impurity is silica, which would be nearly invisible in organic solvents with a similar index of refraction.

A stock solution of HDU-35 (2 wt %) was prepared by adding the required quantity of deionized water to the purified polymer and mechanically agitating the mixture gently for 2 days. The solution was clear. The stock solution was diluted with distilled and deionized water to make 0.05−1.2 wt % solutions that were stirred overnight before performing the experiments. All solutions were kept in the dark at room temperature.

Pyrene (Aldrich) was recrystallized from ethanol and twice sublimed. Ethylpyrene (Molecular Probes) was used as received. Distilled water was further purified through a Millipore Milli Q purification system.

UV Absorption Measurements. A Hewlett-Packard 8452A diode-array spectrophotometer was used. In all measurements, a background correction was made by taking a probe-free polymer solution with the same polymer concentration as a

reference. The probe partitions between polymer domains and water. For most of the solutions we examined, the contribution to the optical density by the probe in the water phase was negligible because of its much lower concentration and lower extinction coefficient at the excitation wavelength in comparison to the probe solubilized by the polymer. The concentrations of the micellized probes were calculated from the absorption readings using the following values of the extinction coefficients ϵ: pyrene (3.70×10^4 M^{-1} cm^{-1}, 338 nm) and ethylpyrene (2.34×10^4 M^{-1} cm^{-1}, 346 nm). The extinction coefficients for pyrene and ethylpyrene were determined from UV absorption measurements at high concentrations of polymer where virtually all of the dye is incorporated into a micellar phase. The ϵ value for pyrene determined here is very close to the value determined by Yekta et al. for pyrene solubilized in a similar telechelic associating polymer.[9,10]

Static Fluorescence Measurements. A SPEX Fluorolog 2 spectrometer with double-grating monochromators was used for measurements of pyrene fluorescence (resolution, 0.5 nm; integration time, 1 s). A Perkin-Elmer LS 50B luminescence spectrometer with a resolution of 1 nm was used for measurements of ethylpyrene fluorescence. For pyrene, the excitation wavelength λ_{ex} was 338 nm; for ethylpyrene, λ_{ex} was 346 nm. Nearly all measurements were carried out on aerated solutions. From pyrene emission spectra, two intensity ratios were calculated: the ratio of the first vibrational band (at 371.5 nm) to the third band (at 383 nm) (I_1/I_3) and the ratio of the maximum of the excimer emission (480 nm) to the maximum in the monomer emission (371.5 nm) (I_E/I_M). For ethylpyrene, the maximum of the monomer emission was at 376 nm and the maximum of the excimer emission was at 480 nm.

Probe Saturation Experiments. An excess amount of a probe (0.25 mL of 0.005 M solution in acetone) was deposited on the wall of a centrifuge tube. Acetone was evaporated under a stream of nitrogen, and a polymer solution (2.5−3 mL) was introduced into the tube. The quantity of the dye (75 μmol) is at least a 100 times in excess of the saturation limit for the polymer concentration range studied (0−1.2 wt %). The solutions were stirred for 4 days. Then the excess probe was removed by centrifugation for 40 min at 15000 rpm, and UV absorption spectra were taken. To make sure that saturation had been reached, the solutions were returned to the centrifuge tubes and stirred for 1 more day, and the centrifugation and UV measurements were repeated. The absorption did not change, indicating that the solutions were saturated with the probe. For each solution, excitation spectra were recorded at the monomer emission wavelength (371.5 nm for pyrene and 376 nm for ethylpyrene) and at the excimer emission wavelength (480 nm). When compared, the two excitation spectra show no difference, implying the lack of ground-state preassociation of the probe and successful removal of the excess probe crystals.[22]

For concentrations greater than 2 wt % another technique of probe solubilization was used. The required amount of 1×10^{-3} M probe solution in CH_2Cl_2 (usually less than the maximum saturation limit as extrapolated from the low-concentration data) was added to the dry purified polymer. Then, additional dichloromethane (spectra grade) was added to the mixture to make a 15−20 wt % solution. This solution was stirred overnight. Next, CH_2Cl_2 was removed on a rotary evaporator. The resulting mixture is a homogeneous "solid solution" of pyrene in HDU with a fixed pyrene-to-polymer ratio. Different portions of this mixture were put in small test tubes, and deionized water was added to obtain the desired concentration of the polymer. The test tubes were sealed with Parafilm and a plastic cap, and the mixture was allowed to swell overnight. To ensure full mixing, the test tube was placed into the centrifuge with the empty end down and then centrifuged for 15 min at 5000 rpm. When the centrifuge stopped spinning, the test tube was turned over and the operation was repeated four times. Next, the solutions, which were clear and slightly opalescent, were allowed to sit for at least 1 week before measurements were carried out. All solutions were stored in the dark at room temperature.

Dynamic Fluorescence Measurements. Fluorescence decay profiles of the probe monomer emission were measured using the single-photon-timing technique.[23] Data were collected to a maximum of 20000 counts in the most intense channel. In this technique, the measured decay profile is a convolution of the true decay and the instrument response function. To determine the instrument response function, the mimic technique[24] was employed, using *p*-bis-[2-(5-phenyloxazyl)]benzene in degassed cyclohexane as the reference compound with a lifetime of 1.1 ns.

For each polymer concentration, a series of "dilution" experiments were made. The probe concentration was changed in the following way, while keeping the polymer concentration constant. Initially, the decay profiles were taken for the probe-saturated HDU solutions. Then, an aliquot of solution was removed from the fluorescence cell and the same amount of probe-free polymer solution was added. The contents of the cell were stirred at least 2 h before each experiment to ensure the complete redistribution of the probe between micelles.

Analysis of Fluorescence Decays. Nonexponential decay profiles were fitted to the Poisson quenching micelle model.[18] This model assumes that each micelle contains a maximum of one excited probe molecule and that quencher molecules are randomly distributed among the polymer micelles according to a Poisson distribution law. Both the probe and the quencher must be completely micellized. The distribution is frozen on the fluorescence time scale (i.e., neither the quencher nor the excited probe can escape the micelle during the lifetime of the excited probe). Our experiments use self-quenching of the pyrene chromophore through excimer formation, so that excited pyrene (Py*) or ethylpyrene (EtPy*) serves as the probe and the ground-state pyrene serves as the quencher. The decay profile is described by the following equation:

$$I_M(t) = I_M(0) \exp[-t/\tau_M - n(1 - \exp(-kt))] \qquad (1)$$

where $I_M(t)$ is the monomer intensity at time t, $I_M(0)$ is the initial intensity, τ_M is the unquenched lifetime of the probe monomer, k is the pseudo-first-order rate constant for self-quenching of the excited monomer through dynamic excimer formation, and n is the mean number of probe molecules per micelle.

The parameter n can be related to the chain-end aggregation number N_R by the following equation:

$$n = [\text{probe}]/[\text{micelle}] = [\text{probe}]N_R/(C_{HDU}q_r) \qquad (2)$$

where q_r is the alkyl chain content of the polymer (in mol of alkyl groups/gram of polymer; q_r is equal to 55.5 μmol/g for HDU) and C_{HDU} is the polymer concentration in g/L. In this equation, the critical micelle concentration is assumed to be negligible compared to the polymer concentrations studied.

Results and Discussion

Partitioning of the Probe. Both pyrene and ethylpyrene are hydrophobic molecules that have very low water solubility. In HDU solutions, however, the probe solubility increases considerably, owing to the transfer of the probe to the hydrophobic core of polymer micelles. The change in the probe environment is reflected in its absorption and fluorescence spectra. Pyrene is a well-known and often-used probe in the study of micelles.[19,25] When pyrene is solubilized by micelles, its (0,0) band in the absorption spectrum is shifted to the red by 2−3 nm, relative to that in water.[26] For HDU micelles, the shift is from 336 nm in water to 339 nm in the micellar phase. Another useful indicator of the probe polarity is the ratio of intensities of the first to the third peaks in the fluorescence emission spectrum of pyrene, I_1/I_3. In water, I_1/I_3 is equal to 1.7, whereas in nonpolar solvents it has values well-below 1 (e.g., in cyclohexane, $I_1/I_3 = 0.58$[27]). In HDU micelles, I_1/I_3 equals 1.22, indicating

Table 1. Partitioning Results for Pyrene and Ethylpyrene Solubilized by HDU Micelles

probe	water solubility, μM	K, L/g	K_v	f_w,[a] at C_{pol} (wt %) 0.4 wt %	0.8 wt %	1.2 wt %
pyrene	0.7	4.8	2.9×10^5	4.95	2.54	1.70
ethylpyrene	0.1	37.2	2.3×10^6	0.67	0.33	0.22

[a] f_w is the fraction of the dye in the water phase, expressed as the percent.

that the probe environment is hydrophobic, but some contact with water still remains. This value is similar to that found for pyrene in nonionic surfactant micelles.[25]

The results described above establish that the probe is associated mostly with micelles. However, there is always a fraction of the probe molecules in the water phase that is in a dynamic equilibrium with the probe in the micellar phase. Information about probe partitioning is essential for calculating the fraction of the probe in the water phase. This knowledge is necessary to verify the applicability of the model used to calculate micelle aggregation numbers.

To determine the partition coefficient of pyrene and ethylpyrene in HDU micelles, four solutions were prepared with a polymer concentration of 0.1, 0.4, 0.8, and 1.2 wt %, each saturated with the probe as described above. The concentrations of the probe in the solution were calculated from the UV absorption measurements. It was found that the micellized probe concentration varies linearly with the polymer concentration for both probes. In this case, a simple model of two-phase partitioning is sufficient to characterize the system.

The partitioning of pyrene between water and micellar phases can be described by the following equation:

$$K = [\text{probe}]_m^{sat}/([\text{probe}]_w^{sat} C_{pol}) \quad (3)$$

where $[\text{probe}]^{sat}$ is the saturated probe concentration in micellar (m) and water (w) phases, C_{pol} (g/L) is the polymer concentration, and K is an equilibrium constant. Partitioning can also be described by the partition coefficient K_v that takes into account the quantities of the probe in the micellar and water phases relative to the phase volumes:

$$K_v = KM_w/Nv_R \quad (4)$$

where M_w is the molecular weight of the polymer (36000), N is the number of moles of hydrophobe per mole of the polymer (2), and v_R is the molar volume of the hydrophobe. For hexadecane $v_R = 0.293$ L/mol.

The fraction of the probe in water f_w can then be calculated as

$$f_w = 1/(1 + KC_{pol}) \quad (5)$$

The equilibrium constants for both probes, as well as the fractions of the probe in the water phase for the three polymer concentrations that were used in the excimer quenching experiments, are listed in Table 1. We see from these results that the probe solubility in water has a strong effect on partition equilibrium. Both pyrene and ethylpyrene prefer the micellar phase. However, at the polymer concentration 0.4 wt %, as much as 5% of pyrene molecules remain in the water phase. For the less water-soluble ethylpyrene, this number is less than 1%.

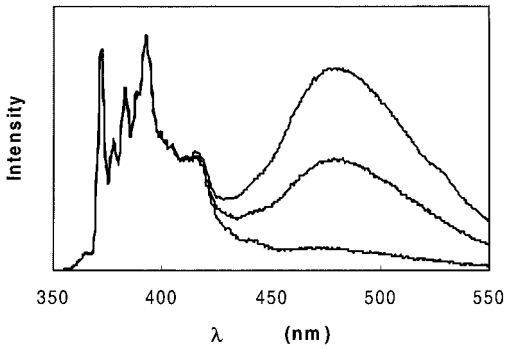

Figure 1. Fluorescence emission spectra of pyrene solubilized in 0.8 wt % HDU solutions; concentration of pyrene, in μM, from top to bottom: 27.0, 16.2, and 2.7. The spectra are normalized at the (0.0) band (371.5 nm).

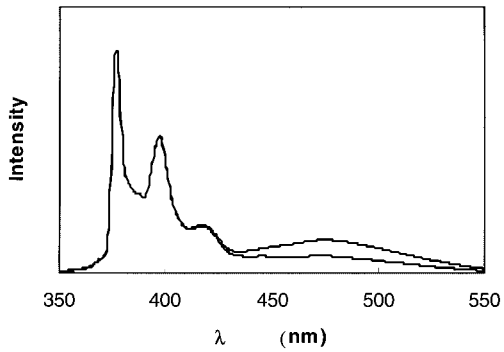

Figure 2. Fluorescence emission spectra of 1-ethylpyrene solubilized in 0.8 wt % HDU solutions; concentration of ethylpyrene, in μM, from top to bottom: 24.5 and 5.8. The spectra are normalized at the (0,0) band (376 nm).

Steady-State Fluorescence Spectra. Steady-state fluorescence spectra for both pyrene and ethylpyrene, solubilized in associative polymer micelles, show similar features (Figures 1 and 2). There are two regions in the spectra: in the 360−430-nm interval, vibrational fine structure is present, and at longer wavelengths, there is a broad structureless band with a maximum at 480 nm. At high concentrations of the chromophore, there is more than one probe molecule occupying the same micelle, and excimer formation is likely. The maximum in the monomer emission in ethylpyrene (376 nm) is red-shifted by 5 nm relative to that of pyrene (371.5 nm). In the ethylpyrene spectrum (Figure 2) the fine structure is not as well-resolved. Part of the difference in the fine structure is due to the poorer resolution of the spectrometer used to measure the ethylpyrene spectra. The ratio of the first-to-third band in the pyrene spectrum is a useful indicator of the polarity of the environment, as described above. The (0,0) transition (first band) is symmetry-forbidden. In polar solvents the probability of the transition is enhanced (the so-called Ham effect[28]). For ethylpyrene, however, this ratio is no longer meaningful, because the symmetry is broken by the ethyl group.

However, the excimer-to-monomer ratio I_E/I_M can be used for both pyrene and ethylpyrene. In Figure 3, the I_E/I_M ratios are plotted against the probe-to-polymer ratio, $[\text{probe}]/C_{pol}$. In this way, one can compare I_E/I_M values for different polymer concentrations. When the data plotted in Figure 3, parts A and B, are compared, one can see that the values of I_E/I_M are always signifi-

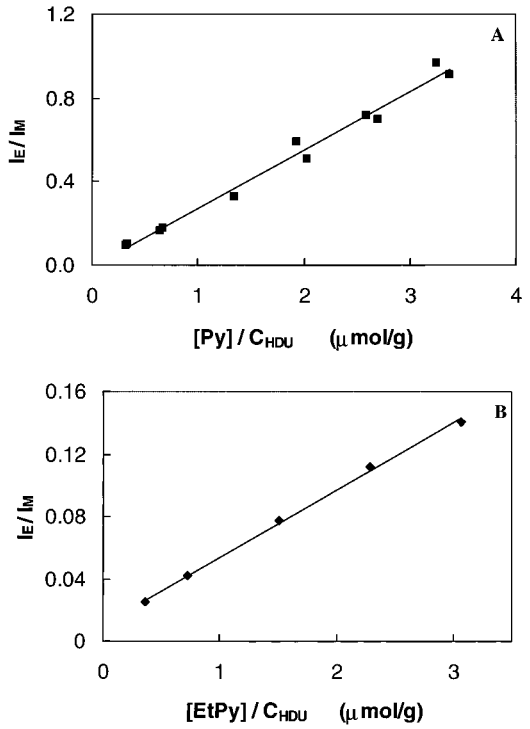

Figure 3. Excimer-to-monomer ratio versus probe-to-polymer ratio. (A) For pyrene in 0.8 and 1.2 wt % HDU solutions. (B) For ethylpyrene in 0.8 wt % HDU solution.

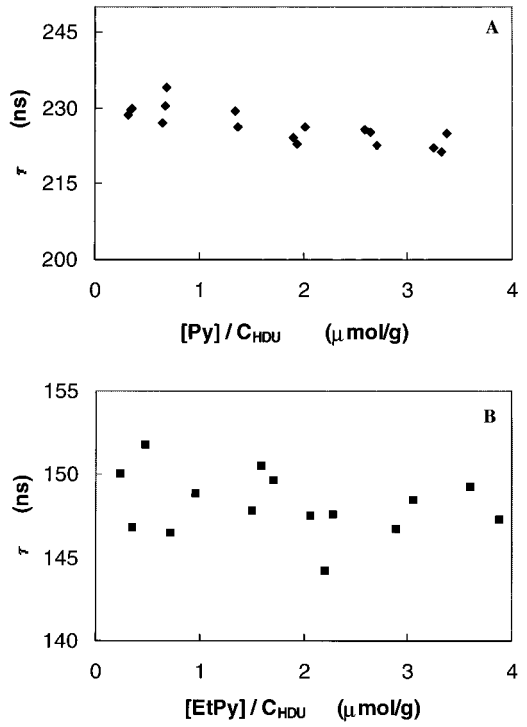

Figure 4. Variation of τ with the probe-to-polymer ratio in HDU solutions (0.4−1.2 wt %). (A) For pyrene. (B) For ethylpyrene.

cantly less for ethylpyrene than for pyrene. For example, in a 0.8 wt % polymer solution, the saturation concentration of pyrene was 27 μM, and the saturation concentration of ethylpyrene was 30 μM. These values are the same within the experimental error. When the corresponding spectra were measured on the same spectrometer (SPEX Fluorolog), I_E/I_M for the pyrene solution was 0.91, and for ethylpyrene, 0.37.

I_E/I_M is a characteristic of the system that can serve as an indicator of a local concentration of a probe in the micelles. When plotted against [probe]/C_{pol}, the excimer-to-monomer ratio is a characteristic feature of a micellar system, provided that the size and aggregation number do not change. For both pyrene and ethylpyrene, I_E/I_M is linearly proportional to the probe-to-polymer ratio.

Analysis of Fluorescence Decay Profiles. The Poisson quenching model (eq 1), widely used for characterizing low-molecular-weight surfactants, has four fitting parameters: $I_M(0)$, the intensity at $t = 0$; τ, the lifetime of an unquenched probe; k, the quenching constant; and n, the average number of quenchers per micelle. In attempting to analyze data with any model, one needs to be sure that the model is adequate for a particular set of data. With nonexponential decay profiles one can always get very good fits to different models provided that the number of fitting parameters is large enough. Proving that a certain model gives a realistic and meaningful description of the system is a much more difficult task. The examination of the fitting-parameter behavior in polymer solutions with different probe contents and different polymer concentrations is useful in screening for abnormalities.

Parameters τ and k. Figures 4A and 5A show the variation of τ and k in HDU solutions when pyrene was used as a probe, and Figures 4B and 5B display similar dependencies for ethylpyrene. Let us consider the behavior of the lifetime τ first. The dependence of the lifetime of the unquenched probe τ with the probe-to-polymer ratio is shown in Figure 4. The data show good reproducibility. For pyrene, the mean lifetime was 227 ± 4 ns, and for ethylpyrene, 148 ± 2 ns. A lack of change in the τ values with the quencher concentration is a sign of the validity of the model assumptions.

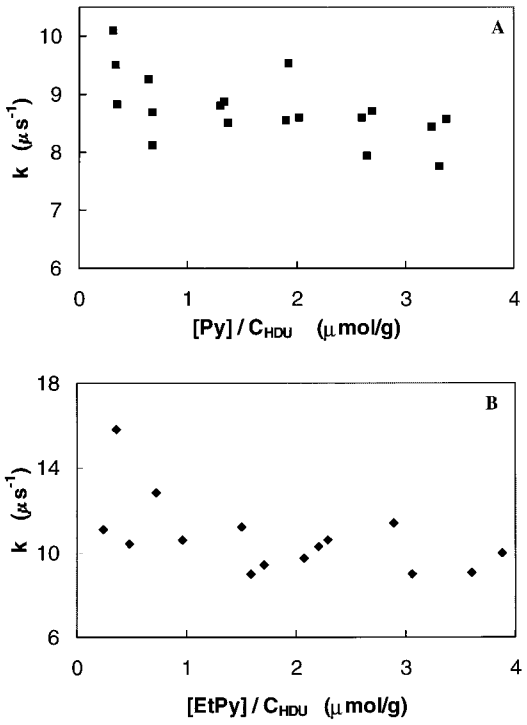

Figure 5. Variation of k with the probe-to-polymer ratio in HDU solutions (0.4−1.2 wt %). (A) For pyrene. (B) For ethylpyrene.

In Figure 5, k is plotted versus the probe-to-polymer ratio. The data show some scatter. The mean value for pyrene, in μs^{-1}, is 8.7 ± 0.6 and for ethylpyrene, 10.4 ±

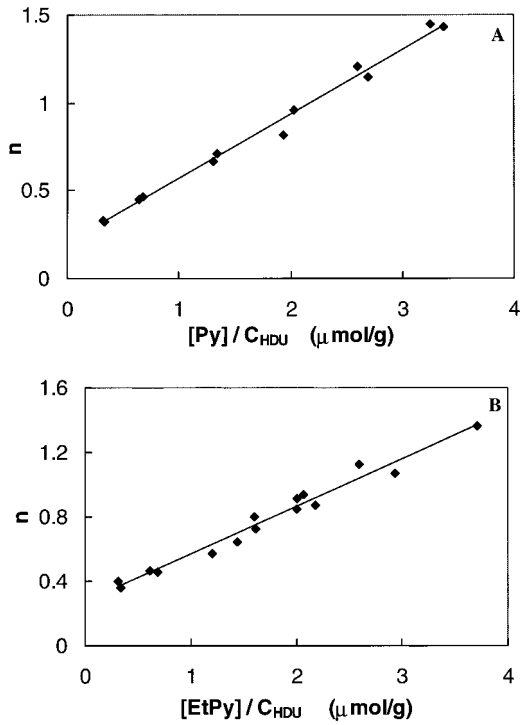

Figure 6. The fitting parameter *n* plotted versus the probe-to-polymer ratio in 0.8 and 1.2 wt % HDU solutions. (A) For pyrene. (B) For ethylpyrene.

1.1. These values are in the range reported by others on similar systems with pyrene as a probe (e.g., 3 μs^{-1} in ref 9 for C_{16}-capped PEOs with $M_n = 26800-51000$ and 20 μs^{-1} in ref 17 for C_{12}-capped PEO, $M_n = 20300$). For part of the pyrene data, we tried to reduce the uncertainty in the *k* and *n* values by fixing the lifetime to 227 ns and fitting the decays with three variable parameters. This approach, however, did not give any improvement in the scatter in the parameters, while producing values very close to the ones obtained with "free" lifetime fits.

Parameter n. The last parameter to be discussed is *n*, the mean number of quencher molecules per micelle. As indicated in eq 2, *n* should vary linearly with the quencher (pyrene or ethylpyrene) concentration and be inversely proportional to the polymer concentration. When *n* is plotted versus the probe-to-polymer ratio, for a system with a constant aggregation number, the plot should yield a straight line that goes through the origin. Figure 6 presents the corresponding plots for pyrene and ethylpyrene in 0.8 and 1.2 wt % polymer solutions. Both plots have similar features. For the two polymer concentrations considered, *n* is a linear function of the probe-to-polymer ratio. For each probe within the experimental error involved, there is no significant difference between the data sets for the two polymer concentrations taken separately. This type of behavior is expected for the case of a constant aggregation number at both polymer concentrations. The unusual feature of the data displayed in Figure 6 is the presence of a nonzero intercept. This feature will be discussed later in some detail.

The aggregation number can be calculated from the slopes of the lines in Figure 6. For pyrene, $N_R = 21 \pm 1$ and for ethylpyrene we find $N_R = 16 \pm 1$. The difference between these numbers is statistically significant and cannot be attributed to random fluctuations only. The contrast between the two probes can be seen better from

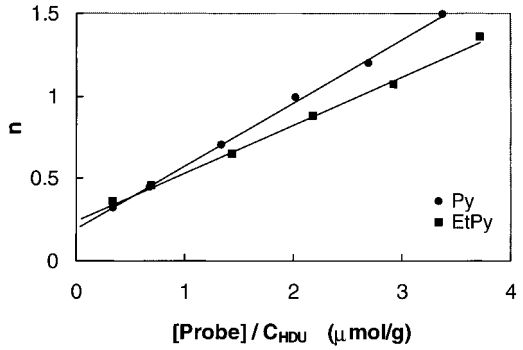

Figure 7. The fitting parameter *n* plotted versus the probe-to-polymer ratio in 0.8 wt % HDU solutions for pyrene ($N_R = 21$) and ethylpyrene ($N_R = 16$).

Figure 7, where *n* is plotted versus the probe-to-polymer ratio for both probes. The pyrene data exhibit a steeper line, corresponding to a higher aggregation number, compared to the ethylpyrene data. We need to consider whether the observed difference between pyrene and ethylpyrene represents a characteristic of the system or is an artifact of the experiment.

One possible explanation can be derived from the fact that one of the assumptions made for the model applied was the assumption of micelle monodispersity (i.e., all micelles have the same size that can be characterized by a unique aggregation number). In reality, however, all surfactants that form micelles do show some degree of polydispersity that may be exaggerated in associative polymers. For example, Alami et al.[17] indicated a possibility of oligomeric aggregates of various sizes in micelles of a hydrophobically modified poly(ethylene oxide) end-capped with $C_{12}H_{25}$ groups. There may be some polydispersity in HDU micelles as well. From the two probes studied, ethylpyrene is the more hydrophobic. A free-energy gain from its solubilization by the micellar core would be greater than that for pyrene. Ethylpyrene, therefore, could be more effectively bound to the smaller micelles, maybe even stabilizing them. In that case, the aggregation number, on the average, would be systematically smaller with ethylpyrene as a probe.

The quenching constant *k* also can be correlated with the size of micelles. In the Poisson quenching model, *k* represents the pseudo-first-order rate constant for quenching of an excited probe in a micelle by a second probe molecule occupying the same micelle. The magnitude of *k* should be proportional to the mobility of the probe in the micelle and inversely proportional to its volume (or size). In larger micelles of comparable microviscosity, on the average, the quenching will take longer and the quenching constant will be smaller. For ethylpyrene, with $N_R = 16$, *k* is 10.4 μs^{-1}, while for pyrene, $N_R = 21$ and $k = 8.7$ μs^{-1}. Although the quenching reactions involved are not exactly the same, the results point in the same direction, that ethylpyrene preferably resides in smaller micelles than pyrene.

Effect of Polymer Concentration on Aggregation Number. In the present set of experiments, we studied HDU solutions over a wide concentration range with pyrene as a probe: from 0.05 to 17 wt %. The high viscosity of these solutions makes it difficult to dissolve pyrene directly in the aqueous polymer solution. Therefore, a new technique was developed where pyrene was predissolved in the polymer before the polymer was dissolved in water. The HDU solutions with high

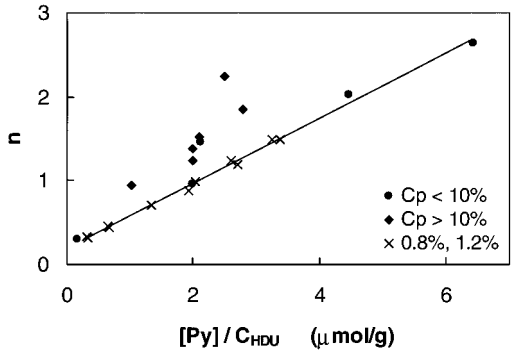

Figure 8. Variation of *n* with the pyrene-to-polymer ratio for HDU solutions with high and low concentrations of the polymer.

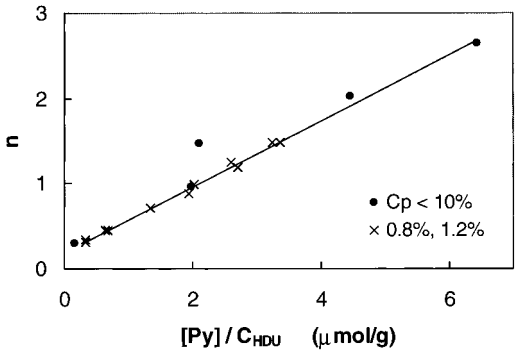

Figure 9. Variation of *n* with the pyrene-to-polymer ratio for HDU solutions with concentrations below 10 wt %.

polymer concentrations and/or high pyrene loading have very high optical densities, even when a 1.0-mm cell is used. As a consequence, a special cell was constructed. It consists of two round quartz plates (25 mm in diameter; 2 mm in thickness) separated by a Mylar spacer with a 120-μm thickness. After a drop of solution was placed between the plates to form a spot of about 1 cm in diameter, the plates were put in a special holder and sealed to prevent water evaporation. After each measurement, the sample was discarded.

UV absorption and fluorescence spectra of the high-concentration solutions did not show any unusual features. There was no ground-state association of pyrene, as confirmed by the comparison of the excitation spectra taken at the monomer and excimer emission wavelengths. Analysis of the fluorescence decay profiles, however, produced some unexpected results. Figure 8 shows the plot of *n* versus the pyrene-to-polymer ratio for high-concentration HDU solutions in comparison to the low-concentration HDU solutions (0.8 and 1.2 wt %). For high polymer concentrations, there is considerable scatter. One can separate the data into two subgroups with respect to the polymer concentration. For HDU concentrations below 10 wt % almost all data points lie close to the trendline for the low-concentration solutions, as shown in Figure 9. At or above 10 wt %, however, the values of *n* become significantly higher, indicating an apparent increase in the aggregation number. This behavior was fairly reproducible. We monitored the solutions for a long time (from 30 to 60 days for some solutions), collecting 3−4 decay profiles for each solution. Estimated day-to-day variation in all fitting parameters was about 5%. For fluorescence emission spectra we obtained similar reproducibility. In Figures 8−10 the mean *n* values are plotted.

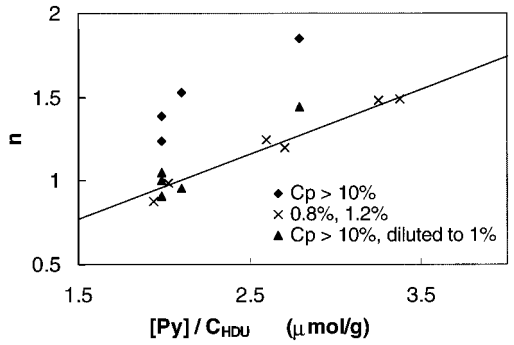

Figure 10. Variation of *n* with the pyrene-to-polymer ratio for HDU solutions with concentrations higher than 10 wt %; diluted HDU solutions and low concentrations of HDU solutions (0.8 and 1.2 wt %).

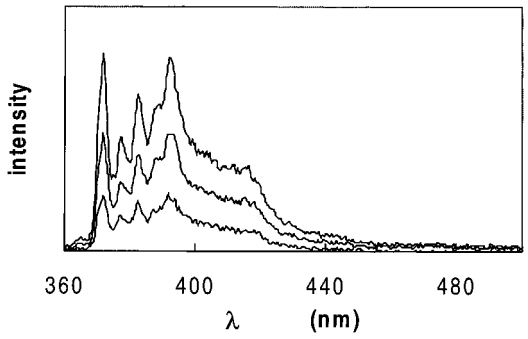

Figure 11. Fluorescence emission spectra of pyrene (0.9 μM) in a 0.2 wt % ODU solution with different oxygen content. Solution equilibrated with, from top to bottom, N_2 , air, and O_2.

To get a better understanding of the observed phenomenon, some of the HDU solutions with polymer concentrations higher that 10 wt % were diluted to yield 1 wt % polymer solutions. An entire set of fluorescence measurements was carried out on the diluted solutions. The *n* values obtained are plotted versus the pyrene-to-polymer ratio in Figure 10. The data for the original high-concentration solutions, and for the 0.8 and 1.2 wt % solutions taken from Figure 6A, are also presented in Figure 10 for comparison. One can see that the *n* values for the diluted solutions are considerably lower than those for the original concentrated solutions. The data points for the diluted solutions fall on the trendline for the low-concentration solutions. This experiment clearly shows the reversibility of the observed changes in *n*.

We can calculate an apparent aggregation number N_a from each *n* value for high-concentration polymer solutions. For well-behaved data, the aggregation number is given by eq 2. Here, we have to introduce a correction for the nonzero intercept, and assume it to be the same for both the high- and the low-concentration solutions (0.2):

$$N_a = (n - 0.2)^* q_r^* C_{pol}/[\text{probe}] \qquad (6)$$

The notation used here is the same as that in eq 2. Calculated in this way, N_a is scattered around a value of 35. For low concentrations, we found an aggregation number of 21. The quenching constant *k* also gives some indication that the size of the micelles changes. As we have already discussed, the quenching constant should decrease with an increasing size of the micelles when the microviscosity of the micelles, or the mobility of the

probe in the micelles, remains the same. For polymer concentrations greater than 10 wt %, k is about 6 μs^{-1}. This is a significant decline from the value of k for low polymer concentration solutions (8.7 μs^{-1}).

At this stage it is too early to try to explain the behavior we observe at high polymer concentrations. We need further experiments and independent evidence to know whether we are observing a peculiarity of the fluorescence quenching experiment or a real change in the micellar structure. Our results are particularly interesting in the light of scattering experiments by François et al.[5] They carried out small-angle X-ray (SAXS) and neutron (SANS) scattering measurements on C_{12} end-capped poly(ethylene oxide)s with various chain lengths. The concentration range was from 2 to 55 wt %. This group observed that a disorder−order transition takes place with the increasing polymer concentration, which they visualized as the organization of spherical micelles into a cubic lattice. These results display an increase in the size of the hydrophobic domains when the polymer concentration is increased. Another report by the same group[6] shows a similar picture for $C_{18}H_{37}$ end-capped polymers.

Nonlinearity of Decay Profiles at Low Probe Concentration. The last matter to be discussed in this paper is the problem we have encountered in analyzing the decay profiles. In Figures 6−10, where n is plotted versus the probe-to-polymer ratio, all plots show a nonzero intercept that is not expected in the model and needs to be accounted for. We begin our analysis of this problem by noting another unexpected feature of the fluorescence decay behavior of the system. Equation 1 predicts that, for micellar systems in the limit of low probe concentration, the fluorescence decay will be a single exponential. We have good reason to anticipate this behavior based upon the stability of fitting the unquenched decay time as shown in Figure 4. Nevertheless, when we measured decay profiles for low probe concentrations at polymer concentrations of 0.8 and 1.2 wt %, the decays were not exponential. This problem is not new: in many associative polymer systems studied by fluorescence techniques, nonexponential decay profiles were observed when, in fact, they should be described by a single-exponential term.[9,17] Some authors did not recognize this as a problem, while others attributed this nonexponentiality to emission from a fluorescence impurity in the polymer and tried to correct for it by adding extra exponential terms to the model equation (eq 1) to describe its decay.[29]

At very low probe concentrations (low probe-to-polymer ratios), the possibility of excimer formation is remote. From the fluorescence spectra in Figures 1 and 2 one can see a significant decrease in the intensity of the excimer emission with a decreasing probe concentration. The plots of the excimer-to-monomer ratio with the probe-to-polymer ratio (Figure 3) are linear and do go through the origin, as expected. Nevertheless, even when the probe concentration is low, the decay profiles show some nonlinearity that results in high values of n. In Figure 6A, where the data for pyrene in low-concentration HDU solutions (0.8 and 1.2 wt %) are displayed, we observe an intercept of about 0.2. This implies that even at low pyrene concentration each micelle contains more quencher molecules (an excess of 1 quencher/5 micelles) than it would if the quenching occurred only by pyrene excimer formation. One way to explain this behavior is to consider how the system would behave if the polymer contained an impurity that could act as a quencher for pyrene fluorescence.

Consequences of an Impurity in the Polymer. The data plotted in Figures 4−6 were obtained by fitting the fluorescence decay profiles to the Poisson quenching model, eq 7.

$$I_M(t) = I_M(0) \exp[-t/\tau_M - n(1 - \exp(-kt))] \quad (7)$$

For two independent quenchers the model would take the form

$$I_M(t) = I_M(0) \exp(-t/\tau_M) \times \exp\{-n_1[1 - \exp(-k_1 t)]\} \exp\{-n_2[1 - \exp(-k_2 t)]\} \quad (8)$$

where the indices 1 and 2 refer to the first and second quenchers Q_1 and Q_2, respectively. Comparing eqs 7 and 8 one obtains:

$$\exp(-kt) = n_1/(n_1 + n_2) \times \exp(-k_1 t) + n_2/(n_1 + n_2) \exp(-k_2 t) \quad (9)$$

Here, we assume that $n = n_1 + n_2$, in other words, that the model as described by eq 7 recovers the correct values of the total numbers of quenchers per micelle. From eq 9 one can show that when

$$n_1 \gg n_2 \qquad k = k_1 \quad (10)$$

and when

$$n_1 \ll n_2 \qquad k = k_2 \quad (11)$$

When the fraction of quencher 1 in the micelles is very low, the quenching rate will be determined by the rate constant of the second quencher, and vice versa. When the fractions of the two quenchers are comparable, the k value would lie between k_1 and k_2. Let us say now that k_1 and n_1 refer to quenching by pyrene, and k_2 and n_2 refer to quenching by an impurity in the polymer so that $[Q_2]/C_{pol}$ is constant for all samples. Looking back at Figure 5A, one can see as that as more pyrene is added to the system and the total number of quenchers n increases, the quenching constant k decreases slightly, so that k_1 is less than k_2, or that the quenching by impurity is more efficient. The same is true for ethylpyrene (Figure 5B).

Identifying an unspecified quencher present in trace amounts in a polymer sample is not an easy matter. It is more straightforward to examine the polymer itself for UV-absorbing or fluorescent impurities, but no such impurities were detected. One possible quencher could be the tin catalyst (dibutyl tin dilaurate) used in the polymer end-capping reaction. This compound is hydrophobic, and one might expect it to associate with the micellar core. A ^{117}Sn NMR experiment measurement was carried out on a concentrated solution of the polymer in $CDCl_3$. The signal was accumulated for 3 days, and no tin was detected.

Consequences of Multiple Sites in the Micelle. An alternative explanation for the nonzero intercept seen in Figure 6 is the possible existence of different solubilization sites for the probe in the polymer micelles. In normal micelles, one imagines that there is a distribution in the probe concentration, from the center to the outer surface of the micelle core. Some probes may be accommodated in the inner layers of the corona as

well. For eq 1 to hold, the probes must redistribute among the various sites on a time scale that is short compared to the fluorescence lifetime. To examine the possibility that the chromophores occupy distinct sites, we will assume that probe molecules in these sites would differ in their kinetic and spectroscopic properties. To simplify matters, let us assume that there are two types of pyrene, "inside" and "outside" pyrenes, and that the exchange rate between them is slow compared to the fluorescence lifetime. Under these circumstances, there will be two distinct lifetimes for these two types of pyrenes, and the decay profile at low probe concentrations will be nonexponential.

One way to test this hypothesis is to expose the system to a different quencher, aiming to obtain different responses for the two pyrene sites. In these experiments, the pyrene concentration must be kept sufficiently low to prevent quenching through excimer formation. One quencher that is already present in a polymer solution is molecular oxygen, which is a very efficient diffusional quencher that, nonetheless, does not interfere with the Poisson quenching kinetics. We can adjust the amount of O_2 by equilibrating the solution with nitrogen gas, or with pure oxygen. This experiment can be carried out at various levels of sophistication. Here, we test for the idea that pyrene in the different sites is characterized by different values of I_1/I_3 and also has different sensitivity to quenching by oxygen. The following set of experiments was carried out to test this idea: A 1 wt % HDU solution with a pyrene concentration of 1.7 mM was prepared and steady-state emission spectra were measured. For solutions degassed by nitrogen bubbling for 15 min, we found an I_1/I_3 ratio of 1.193. For aerated solutions, we found $I_1/I_3 = 1.188$; for solutions in equilibrium with oxygen, $I_1/I_3 = 1.180$. These small changes are reproducible, but not substantially different form one another. These data suggest that as the oxygen concentration increases, the I_1/I_3 ratio of pyrene decreases slightly.

We have carried out preliminary experiments with an analogous polymer containing $C_{18}H_{37}O-$ end groups, which we refer to as ODU. In ODU solutions we also observed nonexponential pyrene decay profiles when the pyrene concentration was low. The effect seen in Figure 6 was somewhat stronger for ODU than for HDU: the intercept in the plot of n versus [Py] is 0.5 (compared to 0.2 for HDU in Figure 6A). Oxygen has a more pronounced effect on the I_1/I_3 ratio of ODU than that of HDU. For a 0.2 wt % ODU solution with [Py] = 0.9 μM, we find $I_1/I_3 = 1.26$ for a deoxygenated solution, and $I_1/I_3 = 1.10$ in an oxygen-saturated solution. These results imply that there is a distribution of pyrene sites in the micelle core, and that pyrene in the more polar environment is somewhat more susceptible to quenching by oxygen.

Summary

We have used pyrene fluorescent probe experiments to study aqueous solutions of the polymer HDU, a poly(ethylene oxide) of $M = 35000$ with $C_{16}H_{33}$ end groups. The end groups were attached by a reaction of the PEO with hexadecyl isocyanate, and the polymer was then purified so that essentially all the polymer in the sample contained 2.0 end groups/polymer molecule. The hydrophobic end groups of this polymer associate in water to form micelle-like structures which serve as solubilization sites for the pyrene molecules. We are particularly interested in the magnitude of N_R, the mean number of end groups per micelle. Fluorescence decay profiles for both pyrene and 1-ethylpyrene were fitted to the Poisson quenching model to obtain the parameters n, the mean number of quenchers per micelle, and k, the pseudo-first-order rate constant for the quenching reaction. While the data seem relatively well-behaved, we obtain different parameters for the two probes. For ethylpyrene, $N_R = 16$ and $k = 10.4\ \mu s^{-1}$, while for pyrene, $N_R = 21$ and $k = 8.7\ \mu s^{-1}$. Plots of n versus [Py] or [EtPy] are linear for various polymer concentrations, but exhibit a nonzero intercept in the limit of a low quencher concentration. We examine a number of possible explanations for this behavior.

Acknowledgment. The authors thank NSERC Canada and the Ontario−Singapore Cooperative Research Program for their support of this research.

References and Notes

(1) (a) *Water-Soluble Polymers: Beauty with Performance*; Glass, J. E., Ed.; Advances in Chemistry 213; American Chemical Society: Washington, DC, 1986. (b) *Polymers in Aqueous Media: Performance through Association*; Glass, J. E., Ed.; Advances in Chemistry 223; American Chemical Society: Washington, DC, 1989. (c) *Hydrophilic Polymers*; Glass, J. E., Ed.; Advances in Chemistry 248; American Chemical Society: Washington, DC, 1996. (d) *Macromolecular Complexes in Chemistry in Biology*; Dubin, P., Bock, J., Davis, R., Schulz, D. N., Thies, C., Eds.; Springer-Verlag: Berlin, 1994.

(2) *Industrial Water Soluble Polymers*; Finch, C. A., Ed.; The Royal Society of Chemistry: Cambridge, U.K., 1996.

(3) Winnik, M. A.; Yekta, A. *Curr. Opin. Colloid Interface Sci.* **1997**, *2*, 424−436.

(4) Rubinstein, M.; Dobrynin, A. V. *Trends Polym. Sci.* **1997**, *5*, 181−186.

(5) Alami, E.; Rawiso, M.; Isel, F.; Beinert, G.; Binana-Limbele, W.; François, J. *Hydrophilic Polymers*; Advances in Chemistry Series 248; American Chemical Society: Washington, DC, 1995; pp 344−362.

(6) François, J.; Maitre, S.; Rawiso, M.; Sarazin, D.; Beinert, G.; Isel, F. *Colloids Surf. A* **1996**, *112*, 251−265.

(7) Persson, K.; Bales, B. L. *J. Chem. Soc., Faraday Trans.* **1995**, *91* (17), 2863−2870.

(8) Yekta, A.; Duhamel, J.; Adiwidjaja, H.; Brochard, P.; Winnik, M. A. *Langmuir* **1993**, *9*, 881−883.

(9) Yekta, A.; Xu, B.; Duhamel, J.; Adiwidjaja, H.; Winnik, M. A. *Macromolecules* **1995**, *28*, 956−966.

(10) Yekta, A.; Duhamel, J.; Brochard, P.; Adiwidjaja, H.; Winnik, M. A. *Macromolecules* **1993**, *26*, 1829−1836.

(11) Semenov, A. N.; Joanny, J.-F.; Khokhlov, A. R. *Macromolecules* **1995**, *28*, 1066−1075.

(12) Rao, B.; Uemura, Y.; Dyke, L.; Macdonald, P. M. *Macromolecules* **1995**, *28*, 531−538.

(13) Chu, B. *Langmuir*, **1995**, *11*, 414−421.

(14) Raspaud, E.; Lairez, B.; Adam, M.; Carton, J.-P. *Macromolecules* **1996**, *29*, 1269−1277.

(15) Raspaud, E.; Lairez, B.; Adam, M.; Carton, J.-P. *Macromolecules* **1994**, *27*, 2956−2964.

(16) Xu, B.; Li, L.; Yekta, A.; Masoumi, Z.; Kanagalingam, S.; Winnik, M. A.; Zhang, K.; Macdonald, P. M. *Langmuir* **1997**, *13*, 2447−2456.

(17) Alami, E.; Almgren, M.; Brown, W.; François, J. *Macromolecules* **1996**, *29*, 2229−2243.

(18) (a)Yekta, A.; Aikawa, M.; Turro, N. J. *Chem. Phys. Lett.* **1979**, *63*, 543−548. (b) Tachiya, M. *Chem. Phys. Lett.* **1975**, *33*, 289−292. (c) Infelta, P. P.; Grätzel, M.; Thomas, J. K. *J. Phys. Chem.* **1974**, *78*, 190−195.

(19) Zana, R. In *Surfactant Solutions: New Methods of Investigation*; Zana, R., Ed.; Surfactant Science Series; Marcel Dekker: New York, 1987; pp 242−294.

(20) Kalayanasundaram, K. *Photochemistry in Microheterogeneous Systems*; Academic Press: London, 1987.

(21) (a) Almgren, M. *Adv. Colloid Interface Sci.* **1992**, *41*, 9−32. (b) Almgren, M. Grätzel, M., Kalayanasundaram, K., Eds.; *Kinetics and Catalysis in Microheterogeneous Systems*; Surfactant Science Series; Marcel Dekker: New York, 1991; pp 63−113. (c) Zana, R.; Lang, J. *Colloids Surf.* **1990**, *48*, 153−171.
(22) Winnik, F. M. *Chem. Rev.* **1993**, *93*, 587−614.
(23) O'Connor, D. V.; Phillips, D. *Time-Correlated Single Photon Counting*; Academic: New York, 1984.
(24) James, D. R.; Demmer, D. R. M.; Verrall, R. E.; Steer, R. P. *Rev. Sci. Instrum.* **1983**, *54*, 1121.
(25) Kalyanasundaram, K.; Thomas, J. K. *J. Am. Chem. Soc.* **1977**, *99*, 2039−2044.
(26) Wilhelm, M.; Zhao, C.; Wang, Y.; Xu, R.; Winnik, M. A. *Macromolecules* **1991**, *24*, 1033−1040.
(27) Dong, D. C.; Winnik, M. A. *Can. J. Chem.* **1984**, *62*, 2560−2565.
(28) Ham, J. S. *J. Chem. Phys.* **1953**, *21*, 756.
(29) Almgren, M.; Hansson, P.; Mukhtar, E.; van Stam, J. *Langmuir* **1992**, *8*, 2405−2412.

MA980819L